

Institute of Physics, Maria Curie-Skłodowska University,
20-031 Lublin, pl. M. Curie-Skłodowskiej 1, Poland

JAN SIELEWIESIUK*, ALBIN CZUBLA

The phase portraits of a three-membered cycle of enzymatic reactions with repression

Portrety fazowe trójczłonowego cyklu reakcji enzymatycznych z represją

1. INTRODUCTION

We would like to continue the analysis of the dynamical system related to a three-membered cycle of enzymatic reactions. The system is described by the following equations

$$\begin{aligned}\frac{dx_1}{dt} &= \frac{x_3 + kx_2}{1 + x_2^m} - \frac{x_1}{1 + x_3^m} - \frac{kx_1}{1 + x_1^m}, \\ \frac{dx_2}{dt} &= \frac{x_1 + kx_3}{1 + x_3^m} - \frac{x_2}{1 + x_1^m} - \frac{kx_2}{1 + x_2^m}, \\ \frac{dx_3}{dt} &= \frac{x_2 + kx_1}{1 + x_1^m} - \frac{x_3}{1 + x_2^m} - \frac{kx_3}{1 + x_3^m},\end{aligned}\tag{1}$$

where k is the relative rate constant for the backward ($x_3 \rightarrow x_2$, $x_2 \rightarrow x_1$, $x_1 \rightarrow x_3$) reactions and m is a parameter whose physical meaning will be discussed later. We suppose that both parameters m and k are non-negative. The analysis of the system presented in [1] can be applied only at small values of k . In the cycle under consideration, the enzymes which catalyse forward reactions ($x_1 \rightarrow x_2$, $x_2 \rightarrow x_3$ and $x_3 \rightarrow x_1$) are repressed (inactivated) by reagents x_3 , x_2 and x_1 respectively. The enzymes which catalyse backward reactions are

* e-mail: sielew@tytan.umcs.lublin.pl

repressed (inactivated, inhibited) by their substrates. Expressions of the type $x_i / (1 + x_j^m)$ can describe Michaelis-Menten kinetics ($m = 1$), reactions catalysed by allosteric and co-operative enzymes ($m = 2, 3$) [2, 3], processes regulated by the repression of enzymes [4, 5, 6] or processes regulated by membrane signalling [7]. At high values of m such expressions can describe inhibiting interactions between neurones [8, 9].

2. THE MAIN FORMAL FEATURES OF THE SYSTEM

The equations (1) possess the cyclic symmetry. Each of these equations can be obtained from the previous one by cyclic substitution $x_1 \rightarrow x_2 \rightarrow x_3 \rightarrow x_1$. The summation of the left and right hand parts of equations (1) leads to the conclusion that

$$\frac{d}{dt}(x_1 + x_2 + x_3) = 0, \quad (2)$$

and to the conservation law:

$$x_1 + x_2 + x_3 = 3C = \text{const} \quad (3)$$

As it follows from (3) the constant $3C$ is an integral of motion of the dynamical system (1). At the same time, the order of our system can be lowered thanks to conservation law. In such a second order system C can be treated as an additional parameter. So, the system (1) contains actually two independent dynamical variables and its phase portrait is contained in the plane defined by the equation (3).

The dynamical variables of the system (1) represent concentrations of the reagents. This is why we take into consideration for them only non-negative initial values. If any of the variables (e.g. x_1) becomes equal to zero then

$$\frac{dx_1}{dt} = \frac{x_3 + kx_2}{1 + x_2^m} \geq 0 \quad (4)$$

and x_1 increases or remains equal to zero. So, under non-negative initial conditions all of the variables remain non-negative for any time. In other words, the system is positively invariant. The positive invariance of the system (1) confines its phase space to the equilateral triangle, contained in the plane (3) in the first octant of the cartesian coordinate system x_1, x_1, x_1 . It would be useful to trans-

form the coordinate system in order to make possible a two-dimensional presentation of the phase portrait. We transform coordinates in the following way

$$\begin{aligned}
 y_1 &= \frac{1}{\sqrt{2}}(x_2 - x_3), & x_1 &= \frac{2}{\sqrt{6}}y_2 + C, \\
 y_2 &= \frac{1}{\sqrt{6}}(2x_1 - x_2 - x_3), & x_2 &= \frac{1}{\sqrt{2}}y_1 - \frac{1}{\sqrt{6}}y_2 + C, \\
 y_3 &= \frac{1}{\sqrt{3}}(x_1 + x_2 + x_3), & x_3 &= -\frac{1}{\sqrt{2}}y_1 - \frac{1}{\sqrt{6}}y_2 + C.
 \end{aligned} \quad (5)$$

The transformation (5) does not change the scale as well as the position of the coordinate origin. Now the whole phase portrait is contained in the plane y_1, y_2 in the equilateral triangle with the following apices: $(0; \sqrt{6}C)$ $(3C/\sqrt{2}; -3C/\sqrt{6})$ and $(-3C/\sqrt{2}; -3C/\sqrt{6})$ which correspond respectively to $x_1 = 3C$, $x_2 = 3C$ and $x_3 = 3C$. The coordinate y_3 is perpendicular to the plane of the triangle and has a constant value of $\sqrt{3}C$.

Of course, equations (1) can be written in variables y_1, y_2, y_3 (5). Such a transformation results in two quite complex equations for time derivatives of y_1 and y_2 . The third equation is very simple:

$$\frac{dy_3}{dt} = 0 \quad (6)$$

The dynamical system (1) has an obvious point of equilibrium at

$$x_1 = x_2 = x_3 = C \quad (7)$$

or, in new coordinates

$$y_1 = y_2 = 0 \quad (8)$$

which is in the centre of the phase triangle. The approximation of the functions in the right of (1) by linear terms of their Taylor's expansion around the point (7) leads to the following linear system:

$$\begin{bmatrix} \frac{dx_1}{dt} \\ \frac{dx_2}{dt} \\ \frac{dx_3}{dt} \end{bmatrix} = \begin{bmatrix} ka - (k+1)b & -(k+1)a + kb & a + b \\ a + b & ka - (k+1)b & -(k+1)a + kb \\ -(k+1)a + kb & a + b & ka - (k+1)b \end{bmatrix} \begin{bmatrix} x_1 - C \\ x_2 - C \\ x_3 - C \end{bmatrix}, \quad (9)$$

where $a = \frac{mC^m}{(1+C^m)^2}$ and $b = \frac{1}{1+C^m}$. In the new coordinates the system (9) takes the form

$$\begin{bmatrix} \frac{dy_1}{dt} \\ \frac{dy_2}{dt} \end{bmatrix} = \begin{bmatrix} \frac{3}{2} \{ka - (k+1)b\} & \frac{\sqrt{3}}{2} \{(k+2)a + (1-k)b\} \\ -\frac{\sqrt{3}}{2} \{(k+2)a + (1-k)b\} & \frac{3}{2} \{ka - (k+1)b\} \end{bmatrix} \begin{bmatrix} y_1 \\ y_2 \end{bmatrix} \quad (10)$$

Equations (10) are especially convenient for the linear analysis of stability.

The central equilibrium (7) is a stable focus at the low values of C . The focus is unstable (the necessary condition for the existence of autooscillations), if

$$m > \frac{mC^m}{1+C^m} > \frac{k+1}{k} \quad (11)$$

At $k=0$, the relation (11) cannot be satisfied at any finite values of m and C . So, the presence of the backward reactions constitutes an additional necessary condition for the existence of autooscillations. We should note that the physically meaningful fulfilment of the condition (11) is possible only at

$$k > \frac{1}{m-1} \text{ and } m > 1. \quad (12)$$

On the other hand, at infinitely high k that is at irreversible backward reactions, relation (11) can be easily satisfied and the central equilibrium can become an unstable focus. However, in this case it does not mean the existence of autooscillations. At high values of k there are in the system six additional equilibrium points. Three of them are saddle points and the other three are stable nodes. In order to find coordinates of these additional equilibrium points one would have to solve a system of two polynomial equations of the high degree. It is impossible even at $m=2$. So, it is impossible to find analytical expressions for the equilibria coordinates. Instead, we have found numerical solutions,

which allow us to present a qualitative description of the evolution of the system at any values of the parameters k and C .

3. ADDITIONAL EQUILIBRIUM POINTS

Additional equilibrium points appear in the phase space only in the certain range of the parameters. Two parameters k and m appear explicitly in the equations (1). The parameter k expresses the rate of backward reactions in relation to the rate of forward reactions. The parameter m is related to the stoichiometry of interactions of allosteric enzymes with their effectors. Alternatively, this parameter can be related to the stoichiometry of interactions of the repressor proteins with their corepressors. The evolution of the system depends also on the third parameter C which corresponds to the mean concentration of the reagents (3) and does not appear explicitly in equations (1). This parameter can be introduced into equations by reducing the system (1) to a second order system using conservation law (3).

It seems clear that we would not be able to manipulate the parameter m in any thinkable experimental system. Instead, we can deal with systems with different values of m . In contrast to this, one can easily manipulate the parameter C , for example, by adding one of the reagents to the system. We can also figure out an experimental system where some changes in the value of k would be possible.

Numerical solutions of the system (1) and the analysis of the shape of the function $x_i / (1 + x_i^m)$ suggest that system with $m > 2$ is qualitatively very much like that with $m = 2$. We will confine the further discussion of the system (1) to the particular case with $m = 2$. It follows from (11) and (12) that $m = 2$ is the least integer value at which autooscillations are possible.

If we put the right hand part of the first equation of the system (1) equal zero and $m = 2$, we will obtain a square equation for x_2 . Thanks to this, x_2 can be expressed analytically as a function of x_1 and x_3 . For any given pair of values of k and x_1 we can calculate numerically the values of x_2 and the right hand side of the second equation as a function of x_3 . Of course, we accept as coordinates of an equilibrium point the set x_1, x_2, x_3 when the right of the second equation is equal to zero at a given value of k . Alternatively, we can directly solve equations resulting from putting equal to zero the right hand parts of equations (1) using the Newton's method. In this case, one of the equations (1) is replaced by the conservation law (3).

Due to the cyclic symmetry of the system (1), additional equilibria appear simultaneously in three points. The system has the only central point of equilibrium at the values of k and C corresponding to the area below the curve 1 in

Fig.1. At k and C belonging to the curve 1 (Fig.1), the system has three additional points of equilibrium. For k and C from the area lying above the curve 1 there are six additional points of equilibrium. There are no additional equilibria for $k < 12.6372$. At $k \approx 12.6372$ and $C \approx 1.35$ there are three and they disappear at any change in the value of C .

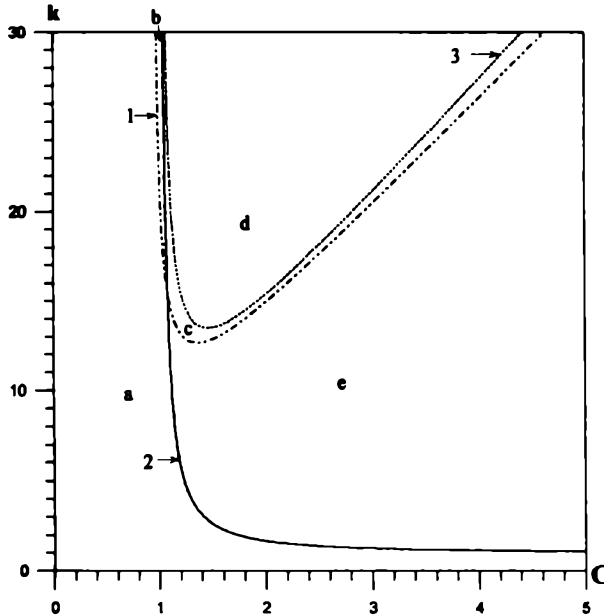


Fig. 1. Bifurcation diagram constructed by using C and k as control parameters at $m = 2$. (curve 1 — saddle-node bifurcation; curve 2 — Hopf bifurcation; curve 3 — heteroclinic orbit bifurcation). The meaning of areas a , b , c , d and e is explained in the text

Diagram bifurkacyjny skonstruowany przy użyciu parametrów kontrolnych C i k przy $m = 2$; (krzywa 1 — bifurkacja typu siodło-węzeł; krzywa 2 — bifurkacja Hopfa; krzywa 3 — bifurkacja orbity heteroklinicznej). Znaczenie obszarów a , b , c , d , e wyjaśniono w tekście

Positions of the additional equilibrium points at $k = 15$ and $k = 50$ are shown in Figure 2 and Figure 3 respectively. Since the linear dimensions of the triangle constituting the physically meaningful phase space are proportional to C , we have used in Figure 2 and Figure 3 reduced coordinates y_1 / C and y_2 / C . The triangle $A_1A_2A_3$ (Fig.2.) can be divided by its heights into six rectangular triangles. Additional equilibrium points appear only in three of these triangles. For given $k > 12.6372$ three additional equilibrium points appear at $C = C_1$. Increasing of C results in the splitting of each of these points into a saddle point and a stable node. Further increasing of C displaces the saddle points toward the centre of the triangle $A_1A_2A_3$. At the same time stable nodes move toward the

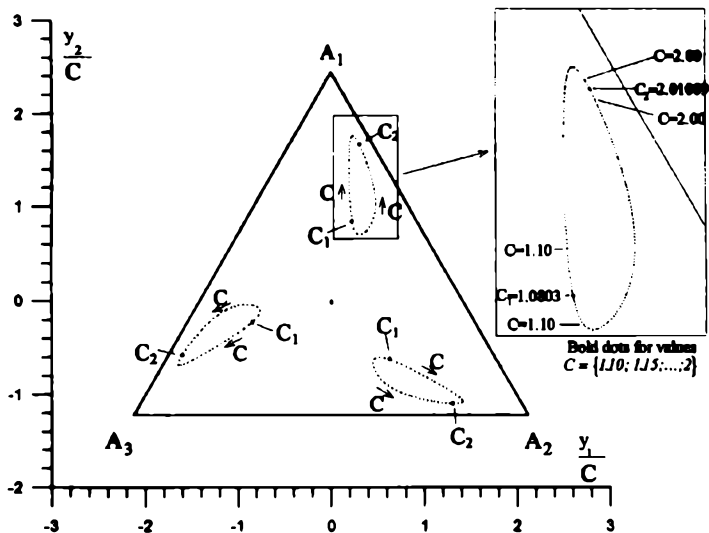


Fig. 2. Positions of the additional equilibrium points at $m = 2, k = 15$ and changing C . There are no additional equilibrium points at $C > C_1$ and $C > C_2$
 Położenia dodatkowych punktów równowagi przy $m = 2, k = 15$ i przy zmieniającym się C .
 W przypadku $C < C_1$ i $C > C_2$ nie ma dodatkowych punktów równowagi

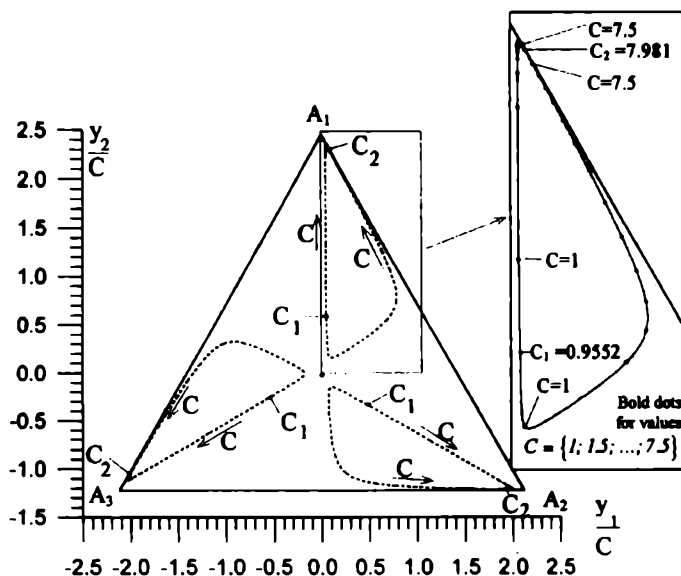


Fig. 3. Positions of the additional equilibrium points at $m = 2, k = 50$ and changing C . There are no additional equilibrium points at $C > C_1$ and $C > C_2$
 Położenia dodatkowych punktów równowagi przy $m = 2, k = 50$ i przy zmieniającym się C .
 W przypadku $C < C_1$ i $C > C_2$ nie ma dodatkowych punktów równowagi

closest apices. Next, the saddle points turn to the middle of the closest side of the triangle $A_1A_2A_3$. At still higher C the saddle points turn once more to the apices of the triangle $A_1A_2A_3$. Finally, the saddle points meet stable nodes at $C = C_2$ and all additional equilibria vanish at $C > C_2$. In this way, at given $k > 12.6372$ additional equilibrium points trace three closed curves as it shown in Figure 2 and Figure 3. At $k = 12.6372$ each of such curves is degenerated to a single point. The higher is the value of k the bigger is the diameter of the curves traced by stable nodes and saddle points in coordinates $y_1 / C, y_2 / C$ at the growing value of C . At very high value of k these equilibrium points move almost along the circumferences of rectangular triangles (compare Fig.3). In the limit case of infinitely high k , when there are in the system only the backward reactions, the coordinates of additional equilibrium points can be obtained analytically. In this case the terms which do not contain k can be omitted in the right of (1). At $m = 2$ the equilibrium can be found as the solution of the equations (13):

$$\begin{cases} (x_2 - x_1)(1 - x_1x_2) = 0 \\ (x_3 - x_2)(1 - x_2x_3) = 0 \\ x_1 + x_2 + x_3 = 3C \end{cases} \quad (13)$$

different from the solution $x_1 = x_2 = x_3 = C$, which are:

$$x_1 = \frac{3C \mp \sqrt{9C^2 - 8}}{2}, \quad x_2 = \frac{3C \pm \sqrt{9C^2 - 8}}{4}, \quad x_3 = \frac{3C \pm \sqrt{9C^2 - 8}}{4} \quad (14)$$

where upper signs correspond to the saddle point and lower signs correspond to the stable node. The other two pairs of equilibrium points can be obtained from (14) by circular substitutions $x_1 \rightarrow x_2 \rightarrow x_3 \rightarrow x_1$. In this case, three additional equilibria appear at $C = \sqrt{8/9}$ on the heights of the triangle $A_1A_2A_3$ between the centre and apices of this triangle in a distance of $1/\sqrt{3}$ from the centre. At increasing value of C , the stable nodes move towards the apices and saddle points move toward the centre of the triangle. At $C = 1$, the saddle points coincide with the centre of the triangle. Simultaneously, at the same value of C the central equilibrium changes its character from stable to unstable focus. On further increasing of C , the stable nodes tend to attain the apices of the triangle and saddle points are moving toward the middles of its sides.

4. AN EXEMPLARY SYSTEM WITH $m = 2$ AND $k = 15$

Let us to follow changes in the phase portrait of the system (1) which take place at the increasing value of parameter C .

As it follows from (11), for

$$C < \sqrt{8/7} \approx 1.069 \quad (15)$$

the central equilibrium point is a stable focus. Moreover, this is the only equilibrium of the system. So, all of the phase trajectories approach to this point, that is, to the state defined by relations (7) and (8) (see Fig. 4). At $C = \sqrt{8/7}$, the Hopf bifurcation takes place in the central focus. The bifurcation differs somewhat from a standard Hopf bifurcation [10, 11] because the limit cycle is not a circle, but has a shape of a smooth triangle with apices directed to the middles of the edges of the triangle confining the phase space (Fig. 5). When C reaches the value $C \approx 1.0803$, then three additional equilibria appear outside the limit cycle. Each of these points splits at the higher C into a stable node and saddle point. In spite of this, there are possible stable autooscillations provided the initial conditions are in the vicinity of the centre. The rest of the phase space is

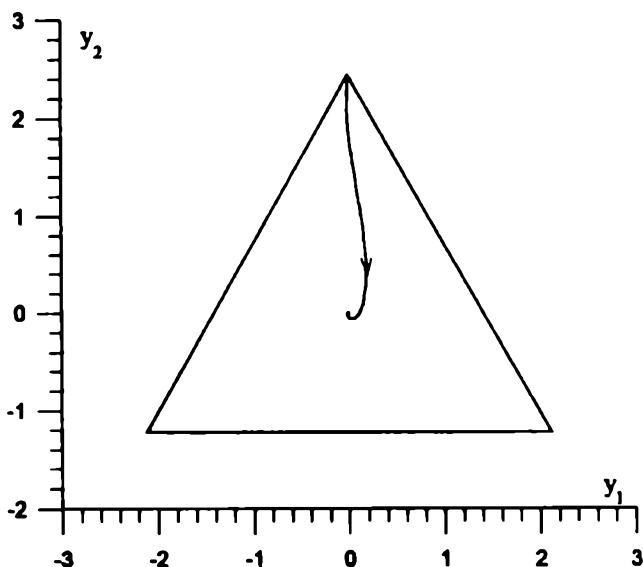


Fig. 4. Phase portrait of the system (1), when there is one stable focus (here $C = 1$, $k = 15$, $m = 2$ — area a in Fig. 1)

Portret fazowy układu (1), gdy w układzie występuje ognisko stabilne (tu $C = 1$, $k = 15$, $m = 2$ — obszar a na Ryc. 1)

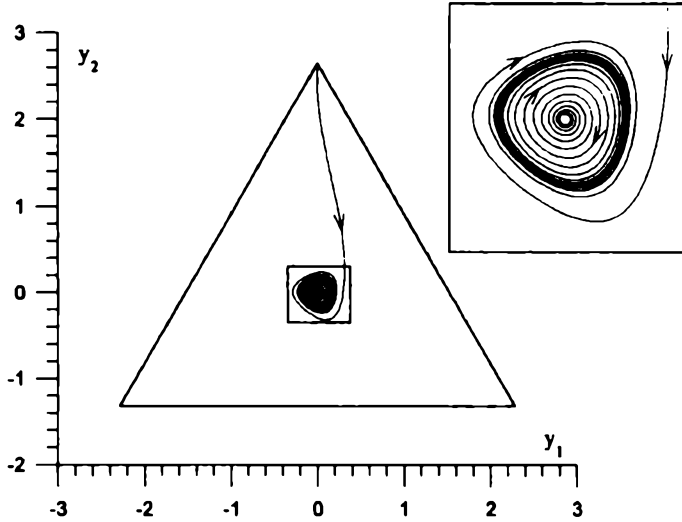


Fig. 5. Phase portrait of the system (1), when there is one unstable focus. Phase trajectories tend to the limit cycle (here $C = 1.079$, $k = 15$, $m = 2$ — area e in Fig. 1)

Portret fazowy układu (1), gdy jedynym punktem równowagi jest ognisko niestabilne. Trajektorie fazowe układu dążą do cyklu granicznego (tu $C = 1.079$, $k = 15$, $m = 2$ — obszar e na Ryc. 1)

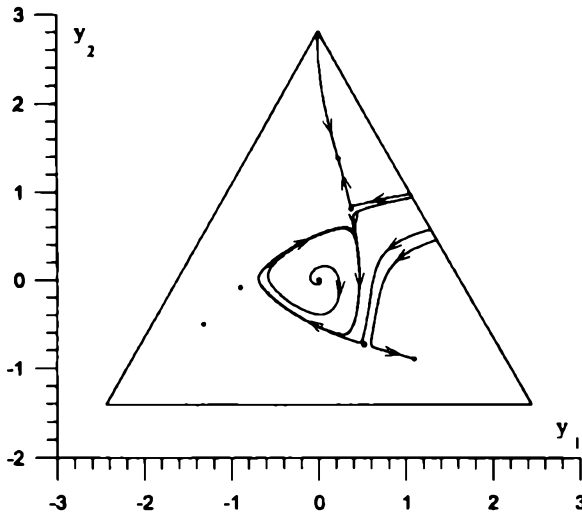


Fig. 6. Phase portrait of the system (1) in the presence of one unstable focus, three saddle points and three stable nodes. Depending on initial conditions, trajectories can tend to the limit cycle or to one of three stable nodes (here $C = 1.15$, $k = 15$, $m = 2$ — area c in Fig. 1)

Portret fazowy układu (1), gdy w układzie występuje ognisko niestabilne, trzy punkty siodłowe i trzy węzły stabilne. W zależności od warunków początkowych trajektorie układu dążą do cyklu granicznego lub do jednego z trzech węzłów (tu $C = 1.15$, $k = 15$, $m = 2$ — obszar c na Ryc. 1)

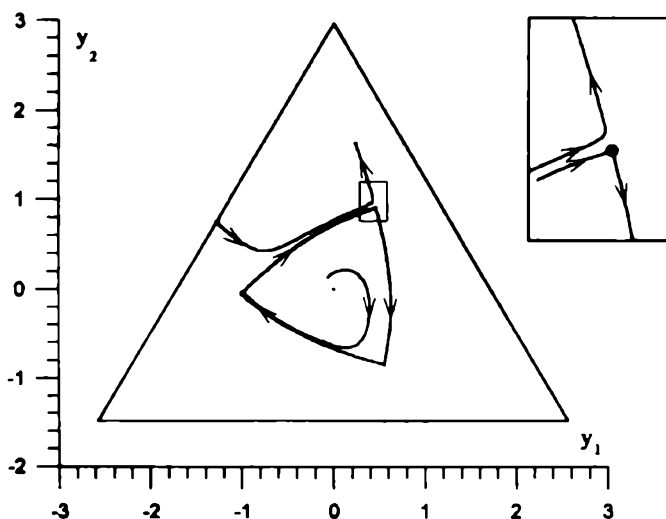


Fig. 7. Phase portrait of the system (1), when the limit cycle changes into a heteroclinic orbit (here $C = 1.211$, $k = 15$, $m = 2$ — the point belonging to the curve 3 in Fig. 1)
 Portret fazowy układu (1) w momencie, gdy cykl graniczny przechodzi w orbitę heterokliniczną (tu $C = 1.211$, $k = 15$, $m = 2$ — punkt należący do krzywej 3 na Ryc. 1)

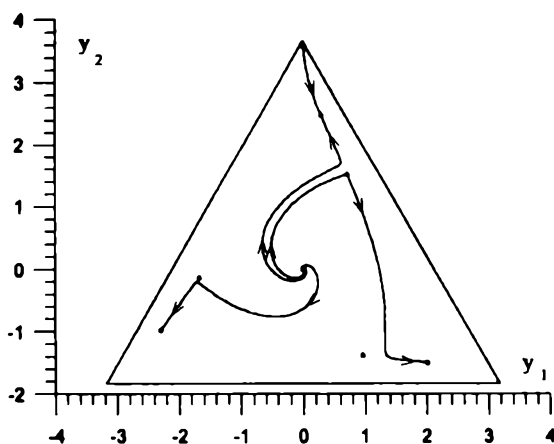


Fig. 8. Phase portrait of the system (1) when there is no limit cycle. The phase trajectories tend to the stable nodes (here $C = 1.5$, $k = 15$, $m = 2$ — area d in Fig. 1)
 Portret fazowy układu (1), gdy nie ma cyklu granicznego. Trajektorie fazowe układu dążą do jednego ze stabilnych węzłów (tu $C = 1.5$, $k = 15$, $m = 2$ — obszar d na Ryc. 1)

divided into three areas of attraction of the three stable nodes (Fig. 6). At $C \approx 1.211$ the limit cycle touches the saddle points and changes itself into heteroclinic orbit [10] passing through all three saddle points (Fig. 7). For C belonging to the interval $(1.211, 1.92)$ there are no stable oscillations. The whole phase space is divided into three attraction areas of the three stable nodes (Fig. 8). At $C \approx 1.92$, a heteroclinic orbit appears again (Fig. 9). It has evidently bigger diameter than that shown in Figure 7. At slightly higher C , the saddle points are separated from the closed orbit which becomes again a limit cycle. In the range of $C \approx (1.211, 1.92)$ almost all phase trajectories approach the limit cycle. However, there are small areas in the vicinity of the triangle apices from where phase trajectories approach one of the stable nodes (Fig. 10). At $C \approx 2.0101$ the saddle points and stable nodes join one another and disappear. At $C > 2.0101$ we have again only one equilibrium point — the central unstable focus. In this case, any phase trajectory comes to the limit cycle, independently on the initial conditions (Fig. 11).

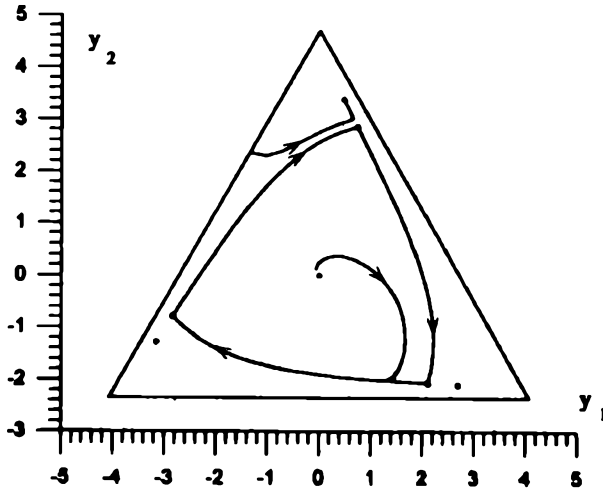


Fig. 9. Phase portrait of the system (1), when a heteroclinic orbit appears again (here $C = 1.92$, $k = 1.5$, $m = 2$ — the point belonging to the curve 3 in Fig. 1)

Portret fazowy układu (1) w chwili, gdy ponownie pojawia się orbita heterokliniczna (tu $C = 1.192$, $k = 15$, $m = 2$ — punkt należący do krzywej 3 na Ryc. 1)

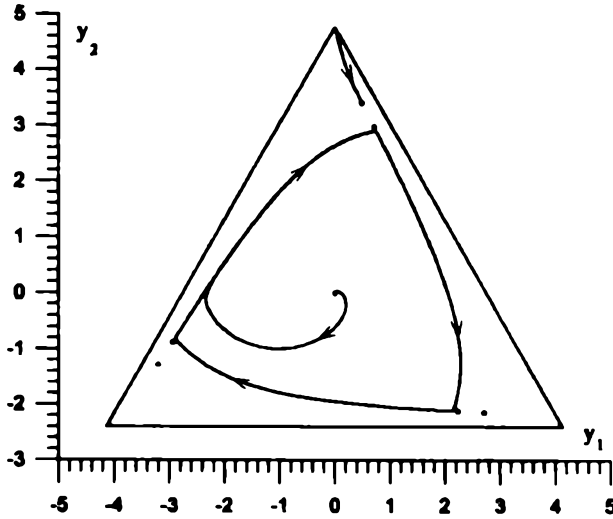


Fig. 10. Phase portrait of the system (1) in the presence of one unstable focus, three saddle points and three stable nodes. Depending on initial conditions, trajectories can tend to the limit cycle or to one of three stable nodes (here $C = 1.95$, $k = 15$, $m = 2$ — area c in Fig. 1)

Portret fazowy układu (1), gdy w układzie występuje ognisko niestabilne, trzy punkty siłowe i trzy węzły stabilne. W zależności od warunków początkowych trajektorie układu dążą do cyklu granicznego lub do jednego z trzech węzłów (tu $C = 1.95$, $k = 15$, $m = 2$ — obszar c na Ryc. 1)

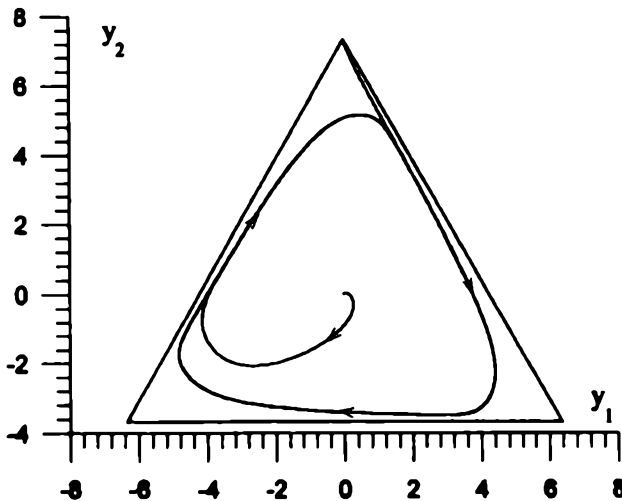


Fig. 11. Phase portrait of the system (1), when there is one unstable focus. Phase trajectories tend to the limit cycle (here $C = 3$, $k = 15$, $m = 2$ — are e in Fig. 1)

Portret fazowy układu (1), gdy jedynym punktem równowagi jest ognisko niestabilne. Trajektorie fazowe układu dążą do cyklu granicznego (tu $C = 3$, $k = 15$, $m = 2$ — obszar e na Ryc. 1)

5. GENERAL VIEW OF THE PHASE SPACE AT $m = 2$

In order to summarise the properties of the dynamical system (1), let us return to Figure 1. which presents the plane of the parameters k and C ($k > 0$, $C > 0$). The C, k plane is divided into five areas by three curves. At values of C and k lying on the curve 1, the system has four points of equilibrium — a focus in the centre of the triangle containing phase space and three double points beyond the centre. This curve has been determined numerically, but its vertical asymptote $C = \sqrt{8/7}$ can be obtained from (10). The system has seven points of equilibrium above the curve 1, that is, in areas b, c and d , and one equilibrium below this curve in areas a and e . The curve 3 corresponds to those values of k and C at which there is a closed heteroclinic orbit passing through three saddle points. This curve has also been constructed on the basis of numerical solutions. The curve 2 corresponds to those values of C and k , at which destabilisation of the central focus or Hopf bifurcation takes place in the system. The curve 2 is a plot of the relation:

$$k = \frac{C^2 + 1}{C^2 - 1}, \quad (16)$$

which can be derived from (11). The curves 2 and 3 have a common vertical asymptote $C = 1$, because at $k \rightarrow \infty$ the saddle points coincide with the centre of the phase space exactly at the same value of $C = 1$, when destabilisation takes place.

We have in Figure 1 the area a which is confined by coordinate axes and the curves 1 and 2. For the parameter values from this area the system evolves towards the only equilibrium (stable focus) at $x_1 = x_2 = x_3 = C$ or $y_1 = y_2 = 0$.

In the area b lying between the curves 1 and 2, (above the curve 1), there exist seven points of equilibrium: stable focus in the centre and three stable nodes and three saddle points beyond the centre. In dependence on the initial conditions, evolution of the system leads to the state $x_1 = x_2 = x_3 = C$ or to one of three stable nodes. Autooscillations are impossible in the area a as well as in the area b . We cannot expect autooscillations also in the area d . In this case the evolution of the system leads to one of three stable nodes (compare Fig. 8). In the area c autooscillations are possible providing that initial conditions are not too far from the centre of the space phase triangle. In the latter case the system evolves towards one of the stable nodes.

In contrast to this, the autooscillations are inevitable in the area e , since there is only one equilibrium — the unstable focus in the centre. Any orbit starting from the vicinity of the centre goes away from this point. On the other hand any

trajectory neither can escape the triangle nor cross itself and there must exist a limit cycle. The necessary Poincaré-Bendixon's criterion [10] for the existence of the closed orbit is satisfied in the areas c , d and e and is not satisfied in the areas a and b .

The lack of analytical expressions for the coordinates of non-central equilibrium points makes impossible to follow in details all bifurcations occurring in the system. In spite of this, we hope that the qualitative description based on numerical solutions would be instructive for understanding what is going on in systems like the one presented by equations (1).

REFERENCES

- [1] J. S i e l e w i e s i u k: *Chemical oscillations in enzymatic cyclic reactions with the conservation of mass*, *Ann. UMCS AAA*, **50/51**, 187–201 (1995/1996).
- [2] J. M o n o d, J. W y m a n, C h a n g e u x, J.-P.: *On the nature of allosteric transitions: a plausible model*, *J. Mol. Biol.*, **12**, 88 (1965).
- [3] J. A. C o h l b e r g, V. B. P i g e t, H. K. S c h a c k m a n: *Structure and arrangement of the regulatory subunits in aspartate transcarbamylase*, *Biochemistry*, **11**, 3396 (1972).
- [4] F. J a c o b, J. M o n o d: *On the regulation of gen activity*. *Cold Spring Harbor Symp. Quantitat. Biol.*, **26**, 193–211 (1961).
- [5] B. C. G o o d w i n: *Oscillatory behaviour in enzymatic control processes*, *Adv. Enzyme Regulation*, **3**, 425–438 (1965).
- [6] B. C. G o o d w i n: *Temporal organisation in cells*, Academic Press., London 1963.
- [7] A. G o l d b e t e r, G. D u p o n t, M. J. B e r r i d g e: *Minimal model for signal-induced Ca^{2+} oscillations and for their frequency encoding through protein phosphorylation*, *Proc. Nat. Acad. Sci. USA*, **87**, 1461–1465 (1990).
- [8] V. L. D u n i n - B a r k o v s k y: *The oscillations of activity level in simple closed neuron chains*, *Biophysica* (Russian) **15**, 374–378 (1970).
- [9] C. A. O r t, W. B. J r. K r i s t i a n, G. S. S t e n t: *Neuronal control of swimming in the medicinal leech. II. Identifications and connections of motor neurons*, *J. Compar. Physiol.*, **A 94**, 121–154 (1974).
- [10] A. H. N a y f e h, B. B a l a c h a n d r a n: *Applied nonlinear dynamics. Analytical, computational, and experimental methods*, John Wiley & Sons, Inc., New York 1995.
- [11] J. D. C r a w f o r d: *Introduction to bifurcation theory*, *Rev. Modern Phys.*, **63**, 991–1037 (1991).

STRESZCZENIE

W artykule dokonano analizy jakościowej dotyczącej dynamiki nieliniowego układu trzech równań, utworzonego w zamkniętym cyklu trzech substancji przekształcających się w siebie kolejno w wyniku reakcji enzymatycznych. Nieliniowe człony występujące w równaniach są typu $1/(1+x^m)$. Dynamikę układu rozważano w zależności od wartości trzech parametrów: m — liczby naturalnej określającej stopień represji syntezy enzymów, k — względnego współczynnika prędkości reakcji wstecznych w stosunku do reakcji w przód; C — średniego stężenia substancji występujących w układzie.

Za pomocą rachunków analitycznych i numerycznych znaleziono w układzie tym trzy różne typy bifurkacji: bifurkację Hopfa, bifurkację typu siodło-węzeł oraz bifurkację orbity heteroklinicznej. Bifurkacja Hopfa prowadzi do pojawienia się w układzie rozwiązań periodycznych. Bi-

furkacja typu siodło-węzeł odpowiada pojawieniu się w układzie trzech dodatkowych punktów równowagi, z których każdy rozdwaja się na siodło i węzeł stabilny. Natomiast bifurkacja orbity heteroklinicznej odpowiada zanikowi lub pojawieniu się rozwiązań oscylacyjnych w wyniku „zderzenia” cyklu granicznego z punktami siodłowymi. Na rycinach przedstawiono przykładowe portrety fazowe dynamiki układu, w przypadku gdy $m = 2$ i $k = 15$ w zależności od wartości pozostałego parametru C .

Analiza układu prezentowana w tym artykule może zostać zastosowana do wyjaśnienia i zrozumienia niektórych zjawisk o charakterze oscylacyjnym, zachodzących w żywych organizmach bądź przy ich udziale.